J|A|C|S
ARTICLES
Published on Web 04/21/2004

Connecting π-Chromophores by σ-P−P Bonds: New Type of Assemblies Exhibiting $\sigma-\pi$-Conjugation

Claire Fave,[†] Muriel Hissler,[†] Tamás Kárpáti,[§] Joëlle Rault-Berthelot,[‡] Valérie Deborde,[†] Loic Toupet,[||] László Nyulászi,*[,§] and Régis Réau*[,†]

Contribution from the Institut de Chimie de Rennes, UMR 6509 and UMR 6510, and the Groupe Matière Condensée et Matériaux, UMR 6626, CNRS-Université de Rennes1, Campus de Beaulieu, 35042 Rennes, France, and Department of Inorganic Chemistry, Budapest University of Technology and Economics, H-1521 Budapest, Gellért tér 4, Hungary

Received December 15, 2003; E-mail: regis.reau@univ-rennes1.fr

Abstract: To study the ability of σ-P−P skeleton to mediate interaction between π-chromophores, 1,1′-biphospholes bearing phenyl or thienyl substituents at the 2,2′ and 5,5′-position have been prepared and studied. These air-stable derivatives are readily available via a "one-pot" synthesis starting from diynes. Theoretical studies and UV−vis data clearly establish that the two π-systems interact via the σ-P−P bridge. This through-bond interaction results in a lowering of the optical HOMO−LUMO gap of the assemblies. The nucleophilic σ^3-P centers of these 1,1′-biphospholes allow chemical modifications of the σ-bridge. These modifications offer further tuning of the optical properties of the assembly. Electrooxidation of the thienyl-substituted 1,1′-biphosphole results in electroactive materials characterized by low optical band gap and reversible p-doping.

Introduction

Understanding and controlling the electronic interactions between individual chromophoric subunits are of fundamental importance for the engineering of organic materials relevant to electronic or optoelectronic applications.[1] Assemblies in which chromophores are connected by π-conjugated spacers,[1a−g] or organized on a σ-scaffold to induce through-space interaction,[1h−j] have been a subject of intense research. In the late 1960s, Hoffmann recognized that the interaction between π-chromophores can effectively be mediated by σ-skeletons,[2a,b] especially those exhibiting high polarizability and low $\sigma-\sigma^*$ gap.[2] The Si−Si bond admirably provides these characteristics and has been used to construct assemblies exhibiting efficient $\sigma-\pi$ conjugation (hyperconjugation). Of particular interest, this conjugated path results in original electronic properties that have been exploited in material science.[3] For example, in oligo(1,1′-siloles) **A** (Figure 1), effective interaction ($\sigma^*-\pi^*$ conjugation) takes place between the Si−Si bridges and the butadienic moieties, making them very attractive chemical sensors for aromatic molecules[3c,d] or highly efficient electron-transporting materials for light-emitting diode materials.[3e,f]

Considering the unique properties of exhibiting $\sigma-\pi$ conjugation, the search for new σ-skeletons able to mediate such unusual electronic interaction is of considerable interest. The comparison of the properties of disilane **B** and diphosphane **C** (Figure 1) suggests that P−P bonds are likely candidates for this purpose. The heteroatom−heteroatom bond strength is somewhat larger in disilane **B** (74 kcal.mol^{-1}) than in diphosphane **C** (61 kcal.mol^{-1});[4a] furthermore, diphosphane **C** absorbs at longer wavelengths than disilane **B** (λ_{max}: **B**, 200 nm; **C**, 220 nm).[4b−d] We have thus explored this possibility with the design of novel assemblies in which two individual π-chromophores are connected by a P−P bridge. In this article, we show that P−P links are excellent σ-scaffolds to mediate

[†] Institut de Chimie de Rennes, UMR 6509, CNRS-Université de Rennes1.
[‡] Institut de Chimie de Rennes, UMR 6510, CNRS-Université de Rennes1.
[§] Budapest University of Technology and Economics.
[||] Groupe Matière Condensée et Matériaux, UMR 6626, CNRS-Université de Rennes1.

(1) (a) Müllen, K.; Wegner, G. *Electronic Materials: The Oligomer Approach*; Wiley-VCH: Weinheim, Germany, 1998. (b) Garnier, F. *Acc. Chem. Res.* **1999**, *32*, 209. (c) Roncali, J. *Chem. Rev.* **1997**, *97*, 173. (d) Tour, J. M. *Acc. Chem. Res.* **2000**, *33*, 791. (e) Bartholomew, G. P.; Bazan, G. C. *Acc. Chem. Res.* **2001**, *34*, 30. (f) Fox, M. A. *Acc. Chem. Res.* **1999**, *32*, 201. (g) Adams, H.; Hunter, C. A.; Lawson, K. R.; Perkins, J.; Spey, S. E.; Urch, C. J.; Sanderson, J. M. *Chem.−Eur. J.* **2001**, *7*, 22. (h) Kim, Y.; Zhu, Z.; Swager, T. M. *J. Am. Chem. Soc.* **2004**, *126*, 452. (i) Meyer, E. A.; Castellano, R. K.; Diederich, F. *Angew. Chem., Int. Ed.* **2003**, *42*, 1210. (j) Adronov, A.; Fréchet J. M. J. *Chem. Commun*. **2000**, 1701.

(2) (a) Hoffmann, R. *Acc. Chem. Res*. **1971**, *4*, 1. (b) Hoffmann, R.; Imamura, A.; Hehre, W. J. *J. Am. Chem. Soc.* **1968**, *90*, 1499. (c) Paddon-Row, M. N. *Acc. Chem. Res*. **1994**, *27*, 18. (d) Gleiter, R.; Schäfer, W. *Acc. Chem. Res*. **1990**, *23*, 369. (e) Paulson, B. P.; Curtiss, L. A.; Bal, B.; Closs, G. L.; Miller, J. R. *J. Am. Chem. Soc.* **1996**, *118*, 378.

(3) (a) Yamaguchi, S.; Tamao, K. *The Chemistry of Organic Silicon Compounds*; Rappoport, Z., Appeloig, T., Eds.; Wiley: New York, 2001; Vol. 3, p 647. (b) Yamaguchi, S.; Jin, R.-Z.; Tamao, K. *J. Am. Chem. Soc.* **1999**, *121*, 2937. (c) Sohn, H.; Sailor, M. J.; Madge, D.; Trogler, W. C. *J. Am. Chem. Soc.* **2003**, *125*, 3821. (d) Sohn, H.; Calhoun, R.; Sailor, M. J.; Trogler, W. C. *Angew. Chem., Int. Ed*. **2001**, *40*, 2104. (e) Sanji, T.; Sakai, T.; Kabuto, C.; Sakurai, H. *J. Am. Chem. Soc*. **1998**, *120*, 4552. (f) Sohn, H.; Huddleston, R.; Power, D. R.; West, R. *J. Am. Chem. Soc*. **1999**, *121*, 29354. (g) Freeman, W. P.; Tilley, T. D.; Liable-Sands, L. M.; Rheingold, A. L. *J. Am. Chem. Soc*. **1996**, *118*, 10457.

(4) (a) Schoeller W. W. *The Multiple Bonds and Low Coordination in Phosphorus Chemistry*; Regitz, M., Scherer, O., Eds.; Thieme Verlag: New York, 1990; p 5. (b) Baudler, M.; Dobblers, J.; Schoener, Ch. P.; Borgardt, M.; Rackwitz, D.; Krause, U. M. *Z. Anorg. Allg. Chem*. **1995**, *621*, 1459. (c) Dillon, M. A.; Spence, D.; Boesten, L.; Tanaka, H. *J. Chem. Phys.* **1988**, *88*, 4320. (d) Iloh, U.; Toyoshima, Y.; Onuki, H. *J. Chem. Phys.* **1986**, *85*, 4867.

10.1021/ja0317067 CCC: $27.50

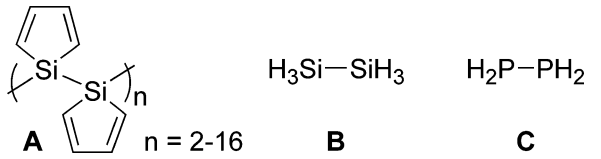

Figure 1. General structure of oligo(1,1′-siloles) **A**, disilane **B**, and diphosphane **C**.

through-bond conjugation and that the possibility to perform chemical modification of the P atoms gives an unique way to tune the electronic properties of the assembly.

Results and Discussion

2,5-Diarylphospholes **2a**,**b** (Scheme 1) exhibit a low HOMO−LUMO gap due to the weak aromatic character of the P ring and the low-lying exocyclic σ^*_{P-Ph} orbital.[5a−e] Solid state data and theoretical studies clearly demonstrate that the extended π-conjugated system in these chromophores involves the two aryl substituents and the butadienic moiety of the phosphole ring.[5a−d] In the present work, derivative **3a** (Scheme 1), assembling such conjugated units via a P−P bond, was prepared according to the classical route to 1,1′-biphospholes.[6a−c] Reductive cleavage of the P−Ph bond of phosphole **2a** afforded an intermediate phospholyl anion (δ ^{31}P NMR, +91.4 ppm), which upon oxidation with iodine gave rise to the target derivative **3a** (Scheme 1) in 69% after purification. Interestingly, 1,1′-biphosphole **3a** is also accessible according to an expedient one-pot synthesis from diyne **1a**, which is the direct precursor of phosphole **2a**.[5c] Subsequent addition of "zirconocene" and an excess of PBr_3 to **1a**[5c] afforded an intermediate 1-bromophosphole (δ ^{31}P NMR, +54.4 ppm) which, in this media, spontaneously provides 1,1′-biphosphole **3a** (Scheme 1).[7] This "one-pot" procedure was used to prepare the 2,2′-5,5′-tetraphenyl-1,1′-biphosphole **3b** (Scheme 1). It appeared to be superior to the classical route to 1,1′-biphospholes since it offers a straightforward multigram scale route to **3a**,**b** from easily accessible diyne precursors.

Derivatives **3a**,**b** are air-stable powders, which have been characterized by high-resolution mass spectrometry and elemental analysis. Their ^{31}P{^{1}H} NMR spectra consist of a singlet at classical chemical shift for 1,1′-biphospholes[6] (δ: **3a**, −0.5 ppm; **3b**, −13.6 ppm). The ^{13}C{^{1}H} data of the carbon skeleton of **3a**,**b** and those of the corresponding phospholes **2a**,**b**[5c] are very similar, except the PC_α signals, which are shielded by ca. 4−5 ppm in **3a**,**b**. Only one set of ^{13}C{^{1}H} and ^{1}H NMR signals could be recorded in CD_2Cl_2 solution between room temperature and −60 °C. These data suggest either a symmetric structure or, as supported by quantum chemical calculations (vide infra), a rapid rotation around the P−P bond. An X-ray diffraction study performed on **3a** (Figure 2) confirmed the proposed structures. The P−P [2.224(1) Å] and P−C [1.802(5)−1.806(5) Å] distances are in the range expected for single bonds.[6e] The P atoms are strongly pyramidalized [Σ bond angles, 293.7°] (Figure 2), with rather acute C−P−P angles [98.37°(15)−105.68°(14)]. The twist angles between two adjacent thienyl and phosphole rings range from 1.2°(5) to 28.6°(8), and the bond lengths and valence angles of the organophosphorus frame of **3a** compare with those of the corresponding 2,5-dithienylphosphole **2a** (Table 1). As observed for the sole other 1,1′-diphosphole characterized by X-ray diffraction study, namely the octaphenyl-1,1′-diphosphole,[6e] the two π-conjugated systems adopt a gauche conformation, with a rather short distance between two C_αP atoms [C1−C28, 3.18 Å] (Figure 2). The sterically disfavored concave topology of **3a** might simply be forced by the packing in the solid state. However, B3LYP/6-31G* calculations reveal that the C_{2h} anti form of **3a** is a saddle point of the PP rotation, by 10.3 kcal/mol higher than the C_2 gauche form. Note that for **3b**, the anti form is also a saddle point at the B3LYP/6-31G* level, by 9.2 kcal/mol higher in energy than the gauche form. These data support a low rotation barrier around the P−P bond in 1,1′-diphospholes **3a**,**b**.

To get more insight into the electronic structure of assemblies of **3a**,**b**, the frontier MOs of the model molecule **3a′**,**b′**, featuring no fused carbocycle, were analyzed. They can basically be derived as the antibonding and bonding combinations of the π-type HOMO and LUMO of the two 2,5-dithienylphosphole moieties. The MOs of **3a′**are shown in Figure 3. First, note that the favored C_2 gauche conformation might be explained by considering a secondary orbital interaction between the HOMO and LUMO at one Cα(P) atom of each conjugated subunits. Second, the splitting in energy of the LUMO and HOMO levels (Figure 3) clearly shows an interaction between the two π-systems.[2a,b] The energy difference between HOMO and HOMO−1 orbitals is small (0.15 eV), since they have a nodal surface at the connecting P atoms, which reduces their interaction. The unoccupied LUMO and LUMO+1 have a larger splitting (0.56 eV) (Figure 3). Furthermore, in contrast to the occupied MOs, the LUMO is the antibonding combination and the LUMO+1 is the bonding combination (Figure 3). This behavior is characteristic for through-bond coupling of two π-systems over an odd number of σ-bonds,[2a,b] which can clearly be seen in the involvement of the σ^*PP and the σPP orbitals (Figure 3). The most important consequence of this through-bond interaction via the P−P bridge on the electronic properties of assembly **3a**,**b** is the narrowing of the HOMO−LUMO gap due the stabilization of the LUMO.

In accordance with the theoretical results, which predict a narrowing of the HOMO−LUMO gap and an increased density of states, the measured absorption spectrum of 1,1′-biphospholes **3a**,**b** differs notably from those of the corresponding phospholes **2a**,**b**. While the spectrum of **2a**,**b** shows only one absorption above 300 nm due to a $\pi-\pi^*$ transition (Figure 4), several bands are recorded for **3a**,**b** with one red-shifted broad shoulder (λ_{onset}: **3a**, 560 nm; **3b**, 460 nm) (Figure 4). The TD-DFT simulated spectra of phospholes **2a**,**b** and 1,1′-biphospholes **3a**,**b**, obtained for the most stable gauche conformer, are shown

(5) (a) Hay, C.; Le Vilain, D.; Deborde, V.; Toupet, L.; Réau, R. *Chem. Commun*. **1999**, 345. (b) Hay, C.; Fischmeister, C.; Hissler, M.; Toupet, L.; Réau, R. *Angew. Chem., Int. Ed.* **2000**, *10*, 1812. (c) Hay, C.; Hissler, M.; Fischmeister, C.; Rault-Berthelot, J.; Toupet, L.; Nyulaszi, L.; Réau, R. *Chem.−Eur. J.* **2001**, *7*, 4222. (d) Delaere, D.; Nguyen, M. T. *Phys. Chem. Chem. Phys.* **2002**, *4*, 1522. (e) Hissler, M.; Dyer, P.; Réau, R. *Coord. Chem. Rev.* **2003**, *244*, 1. (f) Fave, C.; Cho, T.-Y.; Hissler, M.; Chen, C.-W.; Luh, T.-Y.; Wu, C.-C.; Réau R. *J. Am. Chem. Soc.* **2003**, *125*, 9254.

(6) (a) Holand, S.; Mathey, F.; Fisher, J.; Mitschler, A. *Organometallics* **1983**, *2*, 1234. (b) Abel, E. W.; Clark, N.; Towers, C. *J. Chem. Soc., Dalton Trans*. **1979**, 814. (c) Mathey, F. *Chem. Rev.* **1988**, *88*, 429. (d) Quin, L. D.; Quin, G. S. *Phosphorus-Carbon Heterocyclic Chemistry: The Rise of a New Domain*; Mathey, F., Ed.; Elsevier Science: Oxford, 2001. (e) Vohs, J. K.; Wie, P.; Su, J.; Beck, B. C.; Goodwin, S. D.; Robinson, G. H. *Chem. Commun.* **2000**, 1037.

(7) This transformation has been used to prepare nonfunctionalized 1, 1′-bisphospholes, and probably involves the formation of intermediate 1-bromo-1,1′-biphospholium salts, which are reduced by PBr_3: Buzin, F. X.; Nief, F.; Mathey F. Manuscript in preparation.

Scheme 1

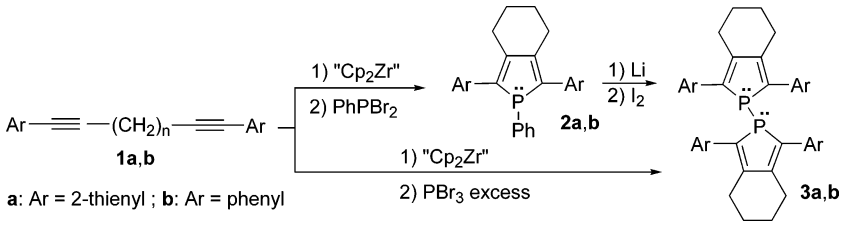

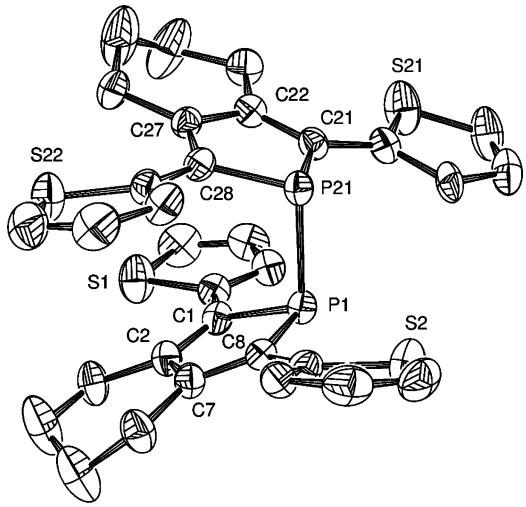

Figure 2. Single-crystal ORTEP structure of **3a**.

Table 1. Comparison of the Solid State Data of Phosphole **2a** and 1,1′-Biphosphole **3a**

	2a[5b]	3a
P1−C1	1.817(4)	1.806(5)
C1−C2	1.366(6)	1.360(7)
C2−C7	1.465(7)	1.459(7)
C7−C8	1.356(6)	1.360(6)
C8−P1	1.818(5)	1.806(5)
C1−P1−C8	90.9(2)	90.8(2)
P1−C8−C7	110.2(4)	110.6(4)
C8−C7−C2	113.9(3)	113.6(4)
C7−C2−C1	114.9(4)	114.7(4)
C2−C1−P1	109.3(3)	110.0(4)

by vertical lines in Figure 4. They fit nicely to the experimental ones (Figure 4), reproducing the changes attributable to the through-bond $\sigma-\pi$ conjugation. For example, the calculated spectrum of **3a** contains two intense transitions at 381 nm (LUMO+1 ← HOMO−1) and 398 nm (LUMO+1 ← HOMO) (experimental values: 361 and 391 nm) and two lower intensity transitions at 479 nm (LUMO ← HOMO−1) and 512 nm (LUMO ← HOMO), corresponding to the broad shoulder (440−560 nm) (Figure 4). These experimental and theoretical results clearly show the crucial role of the σ-P−P bridge in modifying the optical properties of assembly **3a**,**b** by mediating via through-bond interaction between the two π-systems.

It is interesting to note that the UV−vis spectrum of the thienyl-capped **3a** is red-shifted compared to that of the phenyl-substituted **3b**, a trend also observed in the phosphole series **2a**−**b** (Figure 4). The DFT calculated HOMO−LUMO gap is by 0.52 eV smaller in **2a** than in **2b**, and by 0.53 eV smaller in **3a** than in **3b**. These theoretical data suggest that the nature of the substituent on the P ring does not influence significantly the extent of the PP-mediated through-bond interaction in assemblies **3a**,**b**.

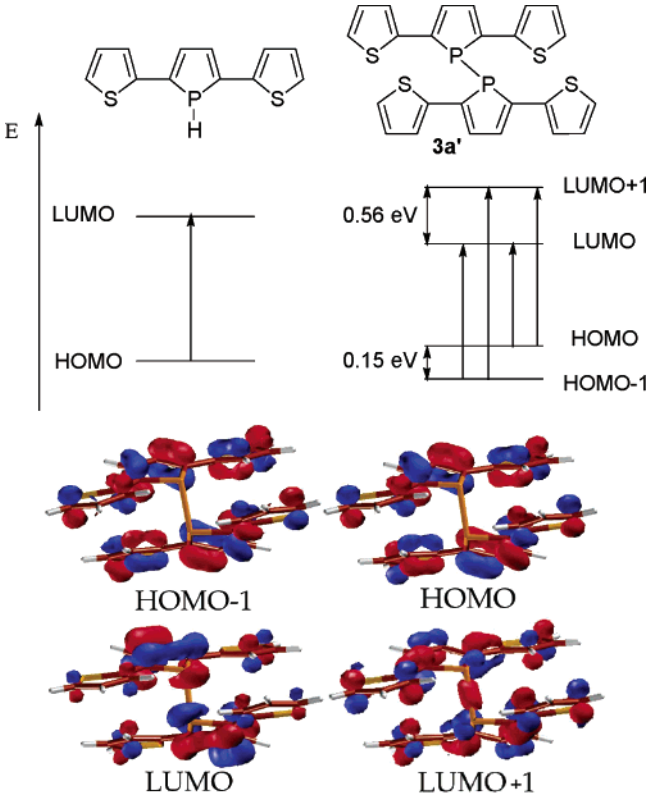

Figure 3. Frontier MOs of the model tetrathienyl-1,1′-diphosphole **3a**′ in its gauche conformation.

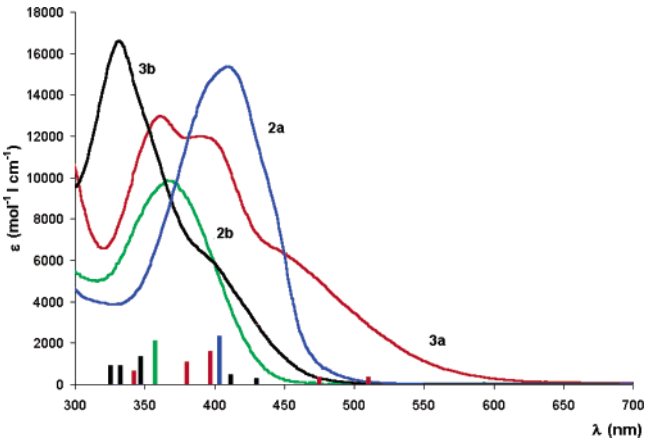

Figure 4. Absorption spectra of **2a**,**b** and **3a**,**b** in CH_2Cl_2 and TD-DFT simulated spectra (vertical lines) of **2a** (in blue), **2b** (in green), **3a** (in red) and **3b** (in black).

Chemical modifications of the P atom of thienyl-capped chromophore **2a** (Scheme 1) offer an unique way to diversify its properties and are key issues for optoelectronic applications of phosphole-based materials.[5f] This fruitful approach has been extended to 1,1′-biphosphole **3a**. Derivatives **4** and **5** are readily

Scheme 2

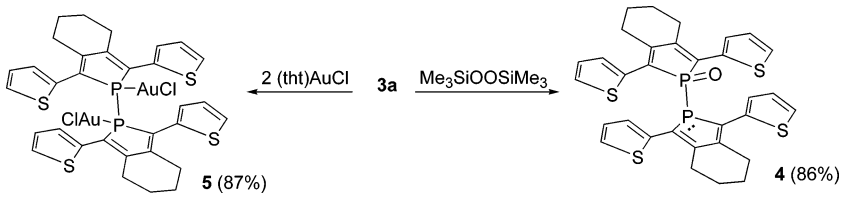

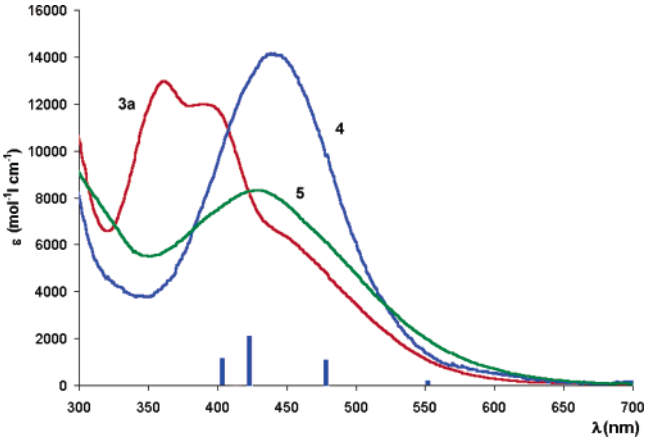

Figure 5. Absorption spectra of **3a, 4** and **5** in CH_2Cl_2 and TD DFT-simulated spectra (vertical lines) of **4** (in blue).

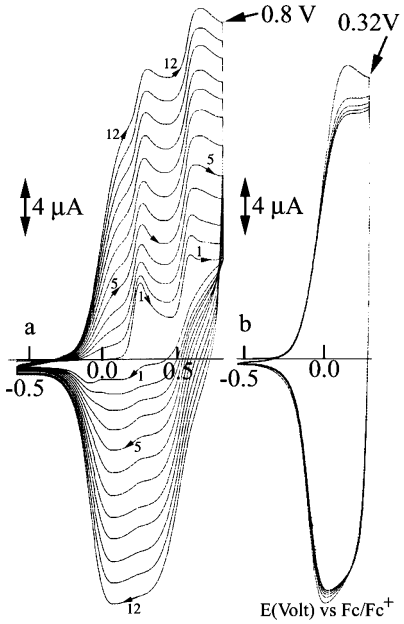

Figure 6. Cyclic voltammograms in dry CH_2Cl_2 containing Bu_4NPF_6 (0.2 M) and Al_2O_3. (a) **3a** (5×10^{-3} M), 12 sweeps between −0.5 and 0.8 V, working electrode: platinum disk (d = 1 mm). (b) Working electrode: platinum disk (d = 1 mm) coated by poly(**3a**) prepared in (a), CH_2Cl_2 solution free of the monomer **3a**, five scans between −0.5 and 0.32 V. Potentials refer to ferrocene/ferrocenium.

obtained according to classical reactions exploiting the nucleophilic behavior of the σ^3,λ^3-P centers of **3a** (Scheme 2). These new derivatives exhibited expected multinuclear NMR data and high-resolution mass spectrum. The dissymmetric nature of **4** is clearly shown by its $^{31}P\{^1H\}$ NMR spectrum consisting in two doublets shielded (−12.5 ppm) and deshielded (+54.5), respectively, compared to the signal of **3a** (−0.5 ppm). The presence of the P−P bond is indicated by the large value of the J_{PP} coupling constant (234.8 Hz). The downfield $^{31}P\{^1H\}$ NMR coordination shift ($\Delta\delta$ (**5**/**3a**), 26.5 ppm) clearly establishes coordination of the P atoms to the gold center,[5f] and the simplicity of the ^{13}C NMR spectrum of **5** favors a symmetric structure. These chemical transformations allow the family of phosphorus-bridged chromophore assemblies to be extended nicely, with three different types of P−P links [(σ^3-P)−(σ^3-P), (σ^3-P)−(σ^4P), (σ^4-P)−(σ^4-P)] being available. Of particular interest, modifying the coordination number of the P centers has an impact on the optical properties of the assemblies. Oxidation of one P center or complexation of the P atoms with gold(I) results in a further bathochromic shift of the band onset compared to 1,1′-biphosphole **3a** (Figure 5). These experimental data are nicely reproduced by TD-DFT calculations performed on derivative **4** (vertical lines, Figure 5). This narrowing of the optical HOMO−LUMO gap strongly suggests that the modified σ-P−P bridges still participate in the interaction of the two π-systems by the hyperconjugative effect. Furthermore, these results nicely illustrate the possible tuning of the optical properties of assembly **3a** via chemical modifications of the P−P σ-skeleton.

One of the most versatile routes toward π-conjugated polymers involves the electropolymerization of thienyl monomers via an oxidation process involving coupling of radical cations.[8] Recently, this process was successfully applied to prepare π-conjugated materials using thienyl-capped phosphole monomers.[5b,c,9] The presence of thiophene termini in **3a** prompted us to investigate its anodic behavior by cyclic voltammetry (CV) on a Pt electrode in CH_2Cl_2 with Bu_4NPF_6 (0.2 M) as the supporting electrolyte. The CV recorded during the first anodic sweep exhibits two irreversible oxidation waves at 0.24 and 0.58 V (ref. ferrocene/ferrocenium, Fc/Fc^+), respectively (Figure 6a). Cycling in a potential range, including only the first wave, does not lead to any modification of this irreversible oxidation wave. In contrast, when scanning in a potential range, including the second wave (i.e., between −0.5 and 0.8 V), the CVs show the appearance and the regular growth of a new reversible wave with a threshold potential at about −0.35 V (Figure 6a). These data indicate that a film is formed on the electrode as a consequence of electropolymerization involving the terminal thiophene groups. The shape of the new anodic wave and the regular growth of the two initial anodic peaks (no shift to more positive potentials and no decrease in intensity) along the recurrent sweeps indicate the conductivity of the deposit. The electrode modified by poly(**3a**) obtained after the 12th sweep was rinsed with dichloromethane and then studied in a new electrolytic solution free of any electroactive species. Poly(**3a**) exhibits a stable and reversible p-doping process (five recurrent

(8) (a) Skotheim, T. A.; Elsenbaumer, R. L.; Reynolds, J. R. *Handbook of Conducting Polymers*, 2nd ed.; Dekker: New York, 1998. (b) Nalwa, H. S. *Handbook of Conductive Materials and Polymers*; John Wiley and Sons: New York, 1997. (c) Audebert, P.; Catel, J. M.; Duchenet, V.; Guyard, L.; Hapiot, P.; Le Coustumer, G. *Synth. Met.* **1999**, *101*, 642.
(9) Hay, C.; Fave, C.; Hissler, M.; Rault-Berthelot, J.; Réau, R. *Org. Lett.* **2003**, *19*, 3467.

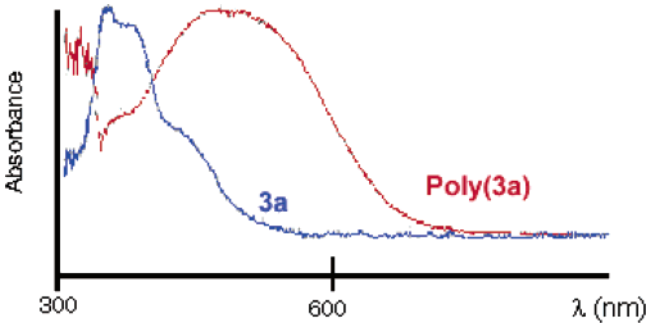

Figure 7. Electronic absorption spectra of **3a** in CH_2Cl_2 and of neutral poly(**3a**) deposited on a platinum concave disk by a potentiostatic oxidation of **3a** at E_{pol} (0.65 V), followed by a reduction of the polymer at 0.0 V. Potentials refer to ferrocene/ferrocenium. Absorbance: arbitrary units.

sweeps between −0.5 and 0.32 V, Figure 6b). The threshold oxidation potential of poly(**3a**) (−0.35 V) is the less anodic encountered in the series of thiophene-phosphole copolymers generated by electropolymerization.[5b,9] Poly(**3a**) can also be readily obtained by potentiostatic oxidation at $E_{pol} = 0.65$ V. It is an insoluble material, hence its thin film absorption spectra was recorded to probe its electronic nature. The material was deposited at E_{pol} on disks of "mirror-polished" platinum and then dedoped at 0.0 V. The UV−vis spectra of poly(**3a**) is considerably red-shifted compared to that of the monomer **3a** (Figure 7). It exhibits a large band with an unresolved maximum at about 594 nm (Figure 7) and a high value of λ_{onset} (730 nm), indicating a narrow optical HOMO−LUMO gap. This result shows that not only molecular species, but also low gap electroactive materials based on 1,1′-biphosphole units, can be readily obtained from **3a**.

Conclusion

The fact that the P−P skeleton is a powerful σ-scaffold to establish through-bond electronic interaction between π-chromophores offers promising perspectives. The σ^*_{P-P} orbital is lower in energy than the σ^*_{Si-Si}, suggesting that P−P bridges can be at least as efficient as the extensively studied Si−Si bridges to mediate $\sigma^*-\pi^*$ conjugation.[10] Furthermore, because of the presence of both reactive P centers and thienyl units, derivative **3a** possesses a high potential in molecular and materials synthesis.

Experimental Section

Materials and Instruments. All experiments were performed under an atmosphere of dry argon using standard Schlenk techniques. Commercially available reagents were used as received without further purification. Solvents were freshly distilled under argon from sodium/benzophenone (tetrahydrofuran, diethyl ether) or from phosphorus pentoxide (pentane, dichloromethane). ^{1}H, ^{13}C, and ^{31}P NMR spectra were recorded on Bruker AM300, DPX200, or ARX400 spectrometers. ^{1}H and ^{13}C NMR chemical shifts were reported in parts per million (ppm) relative to Me_4Si as external standard. ^{31}P NMR downfield chemical shifts were expressed with a positive sign, in ppm, relative to external 85% H_3PO_4. Assignment of carbon atoms was based on HMBC and HMQC experiments. High-resolution mass spectra were obtained on a Varian MAT 311 or ZabSpec TOF Micromass at CRMPO, University of Rennes. Elemental analyses were performed by the CRMPO.

X-ray Diffraction Analyses. Single crystals suitable for X-ray crystal analysis were obtained by crystallization from a dichloromethane/pentane solution of **3a** at room temperature. The unit cell constant, space group determination, and the data collection were carried out on a NONIUS Kappa CCD (with graphite monochromatized Mo Kα radiation ($\lambda = 0.71069$ Å)).[11a] The cell parameters were obtained by fitting a set of 25 high-θ reflections. After Lorentz and polarization corrections, absorption corrections with psi scan,[11b] the structures were solved with SIR-97,[11c] which reveals non-hydrogen atoms of the structure. After anisotropic refinement, all hydrogen atoms were found with a Fourier difference. The whole structures were refined with SHELXL97[11d] by the full-matrix least-squares techniques (use of F magnitude; x, y, z, β_{ij} for C, P, and S atoms), x, y, z in riding mode for the H atoms. Atomic scattering factors were obtained from International Tables for X-ray Crystallography.[11e] ORTEP views were prepared with PLATON98.[11f] All calculations were performed on a Silicon Graphics Indy computer. Crystallographic data (excluding structure factors) for the structures reported in this article were deposited with the Cambridge Crystallographic Data Centre as supplementary publication no. CCDC-225744. Copies of the data can be obtained free of charge on application to CCDC, 12 Union Road, Cambridge CB2 1EZ, U.K. (Fax:(+44)-1223 336−033; e-mail: deposit@ccdc.cam.ac.uk).

Crystal Data for 3a. $C_{64}H_{56}P_4S_8$, $M = 1205.45$, red blocks ($0.12 \times 0.08 \times 0.06$ mm^3). Crystal cell parameters were determined from $\pm\omega$ values of 10 882 reflections and their equivalents in the range $2.66 < \theta < 27.50°$; triclinic, $P\bar{1}$, $a = 10.8103(4)$ Å, $b = 13.6510(5)$ Å, $c = 20.8737(10)$ Å, $\alpha = 94.111(2)°$, $\beta = 91.262(2)°$, $\gamma = 113.140(2)°$, $V = 2821.0(2)$ Å^3, $Z = 2$; density (calcd) = 1.419 g cm^{-3}. Of 10 882 measured reflections, 10882 were independent and 6545 were observed with $I > 2\theta$ (I). R1 = 0.0710, wR2 = 0.1848 for 686 parameters.

Electrochemistry. Cyclic voltammetries were carried out at room temperature with a scan rate of 100 mV/s in a 0.2 M tetrabutylammonium hexafluorophosphate (Bu_4NPF_6) dichloromethane solution. All electrochemical experiments were performed using a Pt disk electrode (diameter 1 mm), the counter electrode was a vitreous carbon rod, and the reference electrode was a silver wire in a 0.1 M $AgNO_3$ CH_3CN solution. Ferrocene was added to the electrolyte solution at the end of a series of experiments. The Fc/Fc^+ couple served as internal standard, and all reported potentials were referenced to its reversible formal potential. All solvents were purchased from SDS, contained less than 100 ppm of water, and were stored under argon. Activated Al_2O_3 was added in the electrolytic solution to remove traces of moisture. The three electrode cells were connected to a PAR model 173 potentiostat monitored with a PAR model 175 signal generator and a PAR model 179 signal coulometer. The cyclic voltammetry traces (CVs) were recorded on an XY SEFRAM-type TGM 164.

Optical Spectra. UV−visible spectra of **2a**, **2b**, **3a**, **3b**, **4**, and **5** were recorded in CH_2Cl_2 solutions at room temperature on a UVIKON 942 spectrophotometer. UV−vis spectra of poly(**3a**) were recorded in dichloromethane solutions using a Guided Wave model 150 spectrophotometer with optical fibers. The polymers were previously deposited on a concave platinum surface that acted as a reflector for the optical beam.[12]

(10) The B3LYP/6-31G* Kohn−Sham LUMO energies of H_3SiSiH_3 and H_2PPH_2 are +0.55 and at −0.32 eV, respectively. The HOMO−LUMO gap of the dithienylsilol (2.96 eV) is smaller than that of dithienylphosphole (3.18 eV). However, the HOMO−LUMO gap of the corresponding 2,2-5,5′-dithienyl-1,1′-silole (2.80 eV) is comparable to that of 2,2-5,5′-dithienyl-1,1′-phosphole **3a′** (2.75 eV).

(11) (a) Fair, C. K. *Molen: An Interactive Intelligent System for Crystal Structure Analysis, User Manual*; Enraf-Nonius: Delft, The Netherlands, 1990. (b) Spek, A. L. *HELENA: Program for the Handling of CAD4-Diffractometer Output, SHELX(S/L)*; Utrecht University: Utrecht, The Netherlands. 1997. (c) Altomare, A.; Burla, M. C.; Camalli, M.; Cascarano, G.; Giacovazzo, C.; Guagliardi, A.; Moliterni, A. G. G.; Polidori, G.; Spagna, R. *J. Appl. Crystallogr.* **1998**, *31*, 74. (d) Sheldrick, G. M. *SHELX97-2: Program for the Refinement of Crystal Structures*; University of Göttingen: Göttingen, Germany, 1998. (e) *International Tables for X-ray Crystallography*; Wilson, A. J. C., Ed.; Kluwer Academic Publishers: Dordrecht, The Netherlands, 1992; Vol. C. (f) Spek, A. L. *PLATON: A Multipurpose Crystallographic Tool*; Utrecht University: Utrecht, The Netherlands, 1998.
(12) Rault-Berthelot, J.; Questaigne, V.; Simonet, J.; Peslerbe, G. *New J. Chem.* **1989**, *13*, 45.

2,2′-5,5′-Tetra(2-thienyl)-1,1′-biphosphole 3a. Method A. To a THF solution (5 mL) of 1-phenyl-2,5-bis(2-thienyl)phosphole **2a**[5b] (0.10 g, 0.26 mmol), Li wire (0.020 g, 2.8 mmol) was added. The solution was stirred for 12 h at room temperature, the excess of lithium was removed, and ^{t}BuCl (28 μL, 0.26 mmol) was added at 0°. The reaction mixture was stirred for 1 h at room temperature, and then a THF solution (5 mL) of iodine (0.067 g, 0.26 mmol) was added. The solution was stirred for 24 h at room temperature, and the volatile materials were removed under vacuo. The solid was poured into CH_2Cl_2 (100 mL), and water (10 mL) and sodium sulfate were added. The organic layer was extracted, and the solvent removed in a vacuum. After purification on alumina (CH_2Cl_2), **3a** was obtained as an air-stable red solid (0.055 g, 69% yield).

Method B. To a THF solution (70 mL) of 1,8-di(2-thienyl)octa-1,7-diyne **1a**[5c] (0.752 g, 2.80 mmol) and Cp_2ZrCl_2 (0.814 g, 2.80 mmol) was added dropwise, at −78 °C, a hexane solution of 1.6 M *n*-BuLi (3.65 mL, 5.80 mmol). The reaction mixture was warmed to room temperature and stirred for 12 h. To this solution was added, at −78 °C, freshly distilled PBr_3 (0.70 mL, 7.50 mmol). The solution was allowed to warm to room temperature and was stirred for 4 days. The solution was filtered on basic alumina, and all the volatile materials were removed under vacuo. The solid was washed with distilled pentane (3 × 10 mL), and **3a** was obtained as a red solid (0.50 g, 60% yield). ^{1}H NMR (300 MHz, $CDCl_3$): δ 1.38 (m, 8H, $=CCH_2CH_2$), 2.30 (m, 4H, $=CCH_2$), 2.45 (m, 4H, $=CCH_2$), 6.86 (m, 4H, H_3 Th), 6.99 (dd, ^3J(H,H) = 5.2 Hz, ^4J(H,H) = 3.7 Hz, 4H, H_4 Th), 7.20 (dd, ^3J(H,H) = 5.2 Hz, ^4J(H,H) = 1.1 Hz, 4H, H_5 Th). ^{13}C−{^{1}H} NMR (75.46 MHz, $CDCl_3$): δ = 22.5 (s, $=CCH_2CH_2$), 28.8 (s, $=CCH_2$), 124.6 (s, C_5 Th), 125.9 (dd, J(P,C) = 6.0 and 5.8 Hz, C_3 Th), 126.9 (s, C_4 Th), 131.1 (d, ^1J(P,C) = 19.3 Hz, PC_α), 139.5 (t-like, J(P,C) = 12.1 and 12.2 Hz, C_2 Th), 144.2 (s, PC_β). ^{31}P−{^{1}H} NMR (121.5 MHz, $CDCl_3$): δ −0.5 (s). HRMS (FAB, *o*NPOE): (*m*/*z*) 602.0549 $[M]^+$, $C_{32}H_{28}P_2S_4$ calcd 602.0549. Anal. Calcd for $C_{32}H_{28}P_2S_4$: C, 63.76; H, 4.68. Found: C, 63.56; H, 4.89.

2,2′-5,5′-Tetraphenyl-1,1′-biphosphole 3b. This compound was prepared according to the above method B using 1,8-di(phenyl)octa-1,7-diyne **1b**[5c] (0.571 g, 2.20 mmol). **3b** was isolated as a yellow solid (0.32 g, 40% yield). ^{1}H NMR (300 MHz, CD_2Cl_2): δ 1.42 (m, 4H, $=CCH_2CH_2$), 1.49 (m, 4H, $=CCH_2CH_2$), 2.40 (m, 8H, $=CCH_2$), 7.23 (d, 8H, ^3J(H,H) = 7.3 Hz, H_2 Ph), 7.31 (dd, 4H, ^3J(H,H) = 7.4 Hz, H_4 Ph), 7.44 (t, 8H, ^3J(H,H) = 7.3 Hz, ^3J(H,H) = 7.4 Hz, H_3 Ph). ^{13}C−{^{1}H} NMR (75.46 MHz, CD_2Cl_2): δ = 22.7 (s, $=CCH_2CH_2$), 27.4 (s, $=CCH_2$), 125.9 (s, C_4 Ph), 127.9 (s, C_3 Ph), 129.3 (s, C_2 Ph), 137.3 (dd, J(P,C) = 9.9 and 8.9 Hz, C_1 Ph), 139.7 (m, PC_α), 144.4 (s, PC_β). ^{31}P−{^{1}H} NMR (121.5 MHz, $CDCl_3$): δ −13.6 (s). HRMS (ESI, CH_3OH): (*m*/*z*) 601.2200 $[M + Na]^+$, $C_{40}H_{36}P_2Na$ calcd 601.2190. Anal. Calcd for $C_{40}HS_{36}P_2$: C, 83.02; H, 6.27. Found: C, 83.36; H, 6.52.

2,2′-5,5′-Tetra(2-thienyl)-1,1′-biphosphole-1-oxyde 4. To a CH_2Cl_2 solution (15 mL) of 1,1′-biphosphole **3a** (0.163 g, 0.27 mmol), neat $Me_3SiOOSiMe_3$ (0.87 mL, 0.27 mmol) was added. The formation of **4** was monitored by ^{31}P NMR spectroscopy. After stirring for 7 days at room temperature, the volatile materials were removed under vacuo, and the residue was washed with diethyl ether (3 × 10 mL). **4** was obtained as a red-brown solid, which can be stored for months under inert atmosphere (0.143 g, 86% yield). ^{1}H NMR (CD_2Cl_2, 300 MHz): δ 1.75−1.85 (m, 8H, $=CCH_2CH_2$), 2.70−2.90 (m, 8H, $=CCH_2$), 7.10 (m, 2H, Th), 7.20 (dd, J(H,H) = 3.8 and 5.2 Hz, 2H, Th), 7.40 (d, J(H,H) = 4.7 Hz, 2H, Th), 7.48 (m, 2H, Th), 7.60 (d, J(H,H) = 3.8 Hz, 2H, Th), 7.65 (m, 2H, Th). ^{13}C−{^{1}H} NMR (CD_2Cl_2, 75.46 MHz): δ 20.8 (s, $=CCH_2CH_2$), 21.6 (s, $=CCH_2CH_2$), 27.0 (d, J(P,C) = 14.4 Hz, $=CCH_2$), 28.6 (s, $=CCH_2$), 124.8 and 125.2 (s, CH Th), 126.2 (d, J(P,C) = 21.5 Hz, PC_α), 126.5 (d, J(P,C) = 4.3 Hz, CH Th), 126.7 (d, J(P,C) = 5.1 Hz, CH Th), 127.0 (s, CH Th), 127.5 (s, CH Th), 135.5 (d, J(P,C) = 17.1 Hz, PC_α or PC_β), 138.7 (d, J(P,C) = 23.9 Hz, C_2 Th), 141.4 (d, J(P,C) = 25.7 Hz, PC_α or PC_β), 147.5 (m, PC_β), one quaternary C_2 Th atom was not observed. ^{31}P−{^{1}H} NMR (CD_2Cl_2, 121.5 MHz): δ +54.5 (d, J(P,P) = 234.8 Hz), −12.5 (d, J(P,P) = 234.8 Hz). HRMS (FAB, *m*NBA): (*m*/*z*) 619.0591 $[M + H]^+$, $C_{32}H_{29}OP_2S_4$ calcd 619.05765.

Gold Complex 5. To a CH_2Cl_2 solution (15 mL) of 1,1′-biphosphole **3a** (0.074 g, 0.12 mmol), neat AuCl(tetrahydrothiophene) (0.079 g, 0.25 mmol) was added. This mixture was stirred for 1 h at room temperature. All the volatile materials were removed under vacuo, and the brown residue was precipated from a CH_2Cl_2 solution (5 mL) by addition of pentane (10 mL). The precipate was washed with pentane (4 × 10 mL) and diethyl ether (4 × 10 mL), **5** was obtained as an air-stable brown solid (0.111 g, 87% yield). ^{1}H NMR (300 MHz, $CDCl_3$): δ 1.49 (m, 8H, $=CCH_2CH_2$), 2.45 (m, 4H, $=CCH_2$), 2.56 (m, 4H, $=CCH_2$), 7.26 (dd, ^3J(H,H) = 5.3 Hz, ^3J(H,H) = 3.6 Hz, 4H, H_4 Th), 7.52 (d, ^3J(H,H) = 3.6 Hz, 4H, H_3 Th), 7.58 (d, ^3J(H,H) = 5.3 Hz, 4H, H_5 Th). ^{13}C−{^{1}H} NMR (CD_2Cl_2, 75.46 MHz): δ 21.5 (s, $=CCH_2CH_2$), 29.1 (d, J(P,C) = 10.0 Hz, $=CCH_2$), 128.0 (d, J(P,C) = 16.4 Hz, PC_α), 128.2 (s, C_4 Th), 128.4 (s, C_5 Th), 129.6 (s, C_3 Th), 134.5 (m, C_2 Th), 150.9 (m, PC_β). ^{31}P−{^{1}H} NMR (CD_2Cl_2, 121.5 MHz): δ +26.0 (s). HR-MS (*m*NBA, FAB): (*m*/*z*) 1030.9553 $[M - Cl]^+$; $C_{32}H_{28}P_2S_4ClAu_2$ calcd 1030.95689. Anal. Calcd for $C_{32}H_{28}P_2S_4Cl_2Au_2$: C, 36.00; H, 2.64. Found: C, 35.84; H, 2.41.

Calculations. Computations were carried out by using the Gaussian 98 program package.[13] For the density functional calculations, the B3LYP hybrid functional was used.[14] The structures were optimized at the B3LYP/3-21G(*) level of theory. Subsequent calculation of the second derivatives showed that real minima (no imaginary frequencies) or first-order saddle points (only one imaginary frequency) was obtained. Further optimization was carried out at the B3LYP/6-31G* level, but at this level no second derivatives were calculated. Time-dependent DFT calculations were performed at the B3LYP/6-31G*//B3LYP/6-31G* level of theory. The MOs shown in Figure 3 are Kohn−Sham MOs, being similar to the canonical HF MOs. The molecular orbitals were visualized by the Molden program.[15]

Acknowledgment. We thank the CNRS, the MNERT, the Conseil Régional de Bretagne (PRIR n° 99CC10), and OTKA T 34675 and D 042216. Support from the Scientific and Technological French−Hungarian Bilateral Cooperation (BALATON program) is also acknowledged.

Supporting Information Available: Crystallographic details (CIF). This material is available free of charge via the Internet at http://pubs.acs.org.

JA0317067

(13) Computations were carried out by using the GAUSSIAN 98 program package. Frisch, M. J.; Trucks, G. W.; Schlegel, H. B.; Scuseria, G. E.; Robb, M. A.; Cheeseman, J. R.; Zakrzewski, V. G.; Montgomery, J. A., Jr.; Stratmann, R. E.; Burant, J. C.; Dapprich, S.; Millam, J. M.; Daniels, A. D.; Kudin, K. N.; Strain, M. C.; Farkas, O.; Tomasi, J.; Barone, V.; Cossi, M.; Cammi, R.; Mennucci, B.; Pomelli, C.; Adamo, C.; Clifford, S.; Ochterski, J.; Petersson, G. A.; Ayala, P. Y.; Cui, Q.; Morokuma, K.; Malick, D. K.; Rabuck, A. D.; Raghavachari, K.; Foresman, J. B.; Cioslowski, J.; Ortiz, J. V.; Stefanov, B. B.; Liu, G.; Liashenko, A.; Piskorz, P.; Komaromi, I.; Gomperts, R.; Martin, R. L.; Fox, D. J.; Keith, T.; Al-Laham, M. A.; Peng, C. Y.; Nanayakkara, A.; Gonzalez, C.; Challacombe, M.; Gill, P. M. W.; Johnson, B. G.; Chen, W.; Wong, M. W.; Andres, J. L.; Head-Gordon, M.; Replogle, E. S.; Pople, J. A. *Gaussian 98*, revision A.5; Gaussian, Inc.: Pittsburgh, PA, 1998.
(14) Becke, A. D. *J. Chem. Phys.* **1991**, *98*, 5648.
(15) Schaftenaar, G.; Noordik, J. H. *J. Comput.-Aided Mol. Des.* **2000**, *14*, 123.